

Double excitation energies from quantum Monte Carlo using state-specific energy optimization

Stuart Shepard,¹ Ramón L. Panadés-Barrueta,^{1, a)} Saverio Moroni,² Anthony Scemama,³ and Claudia Filippi¹

¹MESA+ Institute for Nanotechnology, University of Twente, 7500 AE Enschede, The Netherlands

²CNR-IOM DEMOCRITOS, Istituto Officina dei Materiali and SISSA Scuola Internazionale Superiore di Studi Avanzati, Via Bonomea 265, I-34136 Trieste, Italy

³Laboratoire de Chimie et Physique Quantiques, Université de Toulouse, CNRS, UPS, 31062 Toulouse, France

(*Electronic mail: c.filippi@utwente.nl)

(*Electronic mail: scemama@irsamc.ups-tlse.fr)

(*Electronic mail: moroni@democritos.it)

(*Electronic mail: s.s.shepard@utwente.nl)

(Dated: 26 July 2022)

We show that recently developed quantum Monte Carlo methods, which provide accurate vertical transition energies for single excitations, also successfully treat double excitations. We study the double excitations in medium-sized molecules, some of which are challenging for high level coupled-cluster calculations to model accurately. Our fixed-node diffusion Monte Carlo excitation energies are in very good agreement with reliable benchmarks, when available, and provide accurate predictions for excitation energies of difficult systems where reference values are lacking.

I. INTRODUCTION

An open challenge in computational chemistry is to develop a method which can accurately treat different types of excited states on an equal footing at an affordable cost. An effective way to assess the accuracy of different methods is by comparing vertical transition energies (VTE) with the theoretical best estimates (TBE) determined from high-level computational methods. Environmental effects can influence the measured transition energy in experiment while VTEs calculated using the same molecular geometry are directly comparable.

Conventional single-reference methods, such as time-dependent density functional theory (TD-DFT)¹⁻³ and coupled-cluster theories (CC) (equation-of-motion/linear response⁴), struggle to model double excitations, i.e., excitations whose determinant expansions are dominated by determinants having two orbitals differing from a given reference determinant. The most commonly used, best-scaling, version of TD-DFT uses a linear response formalism which cannot treat multi-electron excitations. A relatively uniform description of singly and doubly excited states relies on workarounds and ad-hoc choices of the exchange-correlation functional.⁵⁻¹⁰

In theory, CC can capture double excitations, but in practice the excitation level must be truncated. For an M -electron excitation, CC must include at least $M+1$ excitations to include a satisfactory amount of correlation,¹¹ but often the $M+2$ level theory is needed to obtain reasonable excitation energies.¹²⁻¹⁶ CC theories needed to treat single and double excitations such as CC3¹⁷ and CCSDT¹⁸ (for singles), and CC4¹⁹ and CCS-

DTQ²⁰ (for doubles) scale poorly with system size as N^7 , N^8 , N^9 , and N^{10} , respectively, limiting their application primarily to small molecules.

Multi-reference methods such as complete active space self-consistent field (CASSCF), CASSCF with a second-order perturbation energy correction (CASPT2),²¹ and the second-order n -electron valence state perturbation theory (NEVPT2)²² are better suited to treat double excitations. Unfortunately, these methods scale exponentially with the number of orbitals and electrons in the active space, limiting them to small active spaces and system size. CASPT2 tends to underestimate the VTEs of organic molecules and a shift is generally introduced in the zeroth-order Hamiltonian to provide better global agreement.²³ These multi-reference methods also rely on chemical intuition to choose which orbitals to include in the active space, but it is often unintuitive which active space will capture the important determinants of a given state.

Selected configuration interaction (sCI)^{24,25} methods are capable of obtaining double excitation energies and have recently been shown to reach full-CI (FCI) quality energies for small molecules.²⁶ Among these approaches is the CI perturbatively selected iteratively (CIPSI)²⁴ method in which determinants are selected based on their contribution to the second-order perturbation (PT2) energy, so that the most energetically relevant determinants are included in the determinant expansion first. This selection criterion both circumvents the excitation-ordered exponential expansion of the wave function used by CI and CC methods and removes the dependence on one's chemical intuition to decide which determinants to include in the expansion.

Quantum Monte Carlo (QMC) methods, specifically, variational (VMC) and fixed-node diffusion Monte Carlo (DMC) are promising first-principles approaches for solving the Schrödinger equation stochastically. These methods scale fa-

^{a)}Current address: Faculty of Chemistry and Food Chemistry, Technische Universität Dresden, 01062 Dresden, Germany

vorably with system size (N^4 with N the number of electrons) and naturally parallelize.^{27–29} In addition, recent improvements in QMC algorithms^{30–33} allow for fast optimization of trial wave functions with thousands of parameters. When using determinant expansions provided by the CIPSI method fully optimized in the presence of a Jastrow factor as trial wave functions, VMC and DMC have been shown to provide accurate excitation energies.^{34–36} The role of the Jastrow factor is to account for dynamic correlations allowing for even shorter determinant expansions.^{37–44}

It is shown here that the same VMC and DMC protocols used previously to calculate single excitations,³⁶ can be used to treat double excitations just as precisely. The pure double excitations of nitroxyl, glyoxal, and tetrazine are calculated using VMC and DMC. In addition, a prediction is made for two excitation energies in cyclopentadienone which have strong double-excitation character in both excited states. The trial wave functions of the ground and excited states are optimized simultaneously, maintaining orthogonality on-the-fly by imposing an overlap penalty.

II. METHODS

In the following, we present how we build the trial wave functions for the QMC calculations, and how we optimize them in VMC energy minimization using a penalty-based, state-specific scheme for excited states, similar to previous approaches.^{45–47}

A. Wave Functions

The QMC trial wave functions take the Jastrow-Slater form,

$$\Psi_I = J_I \sum_{i=1}^{N_{\text{CSF}}} c_{iI} C_i[\{\phi\}_I], \quad (1)$$

where C_i are spin-adapted configuration state functions (CSF), c_{iI} the expansion coefficients, J_I the Jastrow factors, and $\{\phi\}_I$ the one-particle orbitals. In all calculations presented here, the ground and excited states have the same symmetry, so the CSFs, C_i , share the same orbital occupation patterns for all states. Note that each state, I , in Eq. 1 has its own optimal Jastrow factor, set of orbitals, and expansion coefficients. When each state has its own optimizable Jastrow and orbital parameters, the approach is referred to as a state-specific optimization, as opposed to a state-average optimization where all states share a common Jastrow factor and set of orbitals and only the expansion coefficients are state-dependent.^{35,37}

The expansion coefficients and orbitals are initialized for the VMC optimization by one of two methods: (i) a N_{state} -state-average [SA(N_{state})] CASSCF calculation or (ii) a CIPSI calculation, which builds off of approach (i). In approach (i), the SA-CASSCF wave functions are used as starting determinantal components in the VMC optimization (results reported in SI). In approach (ii), one only utilizes the orbitals produced by the SA-CASSCF calculation as the molecular orbital basis

for a CIPSI expansion; in the VMC optimization, the starting determinantal components include the CASSCF orbitals and CIPSI coefficients, c_{iI} .

Alternatively, in approach (ii), the natural orbitals (NO) are calculated from a first CIPSI expansion followed by a second CIPSI calculation in the NO basis. Performing a CIPSI expansion in the NO basis tends to lead to a smoother convergence to lower energies with fewer determinants¹⁴ compared to using a basis of SA-CASSCF orbitals. In other words, one can obtain a higher quality wave function with fewer determinants via relaxation of the molecular orbital basis.

Further details on the CASSCF initial wave functions and CIPSI calculations using the NO basis are provided in the supplementary information (SI).

B. Penalty-Based State-Specific Method

When trying to optimize a state which is not the lowest in its symmetry class, the state can collapse to a lower-energy eigenstate. One way to prevent this is to impose orthogonality between the higher energy state and all states lower in energy. To this end we employ a penalty-based state-specific method which requires minimizing the objective function,⁴⁷

$$O_I[\Psi_I] = E_I[\Psi_I] + \sum_{J \neq I} \lambda_{IJ} |S_{IJ}|^2, \quad (2)$$

where E_I is given by,

$$E_I = \frac{\langle \Psi_I | H | \Psi_I \rangle}{\langle \Psi_I | \Psi_I \rangle} = \langle E_L^I(\mathbf{R}) \rangle_{\mathbf{R} \sim |\Psi_I(\mathbf{R})|^2}. \quad (3)$$

E_L^I is the local energy, $H\Psi_I/\Psi_I$, and $\langle \cdot \rangle_{\mathbf{R} \sim \cdot}$ denotes the Monte Carlo average of the quantity in brackets over the electron configurations, \mathbf{R} , sampled from the indicated distribution (in this case, $|\Psi_I(\mathbf{R})|^2$). The normalized overlap, S_{IJ} , is given by,

$$S_{IJ} = \frac{\langle \Psi_I | \Psi_J \rangle}{\sqrt{\langle \Psi_I | \Psi_I \rangle \langle \Psi_J | \Psi_J \rangle}}. \quad (4)$$

In order to simultaneously sample quantities for multiple states with comparable efficiency, a guiding function, $\Psi_g = \sqrt{\sum_I |\Psi_I|^2}$, is introduced and the energy of a given state (Eq. 3) is estimated as a weighted average

$$E_I = \frac{\langle t_I E_L^I \rangle_{\mathbf{R} \sim \rho_g(\mathbf{R})}}{\langle t_I \rangle_{\mathbf{R} \sim \rho_g(\mathbf{R})}}, \quad (5)$$

where now the configurations are sampled from the distribution, $\rho_g = |\Psi_g|^2$ and the weight t_I is given by $t_I = |\Psi_I/\Psi_g|^2$. Similar weighted averages are calculated for the derivatives of each state (see SI).

The Jastrow, orbital, and CSF parameters of each state are optimized using the stochastic reconfiguration (SR)^{48,49} method. The gradients used in the SR equations are found by taking the parameter derivatives of Eq. 2, also derived in the SI.

In the implementation proposed by Pathak *et al.*, the state being optimized, Ψ_I , is forced to be orthogonal to fixed, pre-optimized, lower-energy states, or anchor states, Ψ_J . Each higher-energy state is then optimized consecutively, imposing orthogonality with all anchor states lower in energy. Each λ_{IJ} in Eq. 2 controls the overlap penalty for the state currently being optimized, Ψ_I , due to each anchor state, Ψ_J , which is suggested to be on the order of, and larger than, the energy spacing between the states.

The method is implemented here such that all states are optimized at the same time, with orthogonality imposed on-the-fly. Since all states are changing from one SR step to the next, the overlap penalty must be imposed between all states. Therefore, ' \neq ' is used in the summation in Eq. 2 instead of '<' so that each state is kept orthogonal to all states, even to those higher in energy. Importantly, in circumstances where states are close in energy, their order may change throughout the optimization and, with ' \neq ' in Eq. 2, the ordering of the states in energy does not need to be known in advance. Finally, the use of correlated sampling in the concomitant optimization of all states reduces the length of the Monte Carlo simulations needed to acquire a given accuracy on the energy differences among the states.

C. Analysis of λ_{IJ} 's effect on energies and VTEs

We illustrate the effect of λ_{IJ} on the optimization of the 3-state cyclopentadienone system with a small CIPSI expansion on CAS orbitals, performing a total of 800 SR iterations for different choices $\lambda^{(i)}$, each corresponding to a different triplet of values $(\lambda_{12}, \lambda_{13}, \lambda_{23})$. In general, we expect that if λ_{IJ} are too small some of the states may lose orthogonality and collapse onto each other; on the other hand, if they are too large, the fluctuations of the overlaps S_{IJ} will be amplified, downgrading the efficiency of the SR minimization because more sampling will be required to pin down the optimal variational parameters at the desired level of statistical precision.

As shown in Figure 1, if all λ_{IJ} are set to zero, the excited states collapse toward the ground-state wave function (left panel), whereas they are bounded by the respective eigenstates with the choice of λ_{IJ} indicated in the right panel.

The selection of suitable values of λ_{IJ} is neither difficult nor critical. Figure 2 shows the overlaps $|S_{IJ}|^2$ and excitation energies (ΔE_{IJ}) for various choices of λ_{IJ} . In panel (a), for $\lambda^{(1)-(4)}$, there is a noticeable increase in the overlaps, while the choices of $\lambda^{(5)-(9)}$ prevent the overlaps from increasing; however, for $\lambda^{(10)}$, $|S_{13}|^2$ tends to be uniformly larger. Panel (b) shows some examples of the correspondence between increasing (stable) overlap and decreasing (stable) gap. Finally, panel (c) shows that all choices $\lambda^{(5)-\lambda^{(9)}}$ are equally good in terms of the final estimate of the excitation energies, whereas for $\lambda^{(1)-\lambda^{(4)}}$ the gaps (particularly ΔE_{13}) are somewhat smaller and may eventually collapse with more SR iterations. In the case of $\lambda^{(10)}$, the signal is stable along the iterations, but the excitation energy E_{13} is somewhat less accurate, than with $\lambda^{(5)-\lambda^{(9)}}$; it could be improved with more sampling per SR step, losing however efficiency.

In conclusion, there is a wide range of λ_{IJ} ($\lambda^{(5)-\lambda^{(9)}}$) where the estimate of the excitation energies is stable, consistent and efficient.

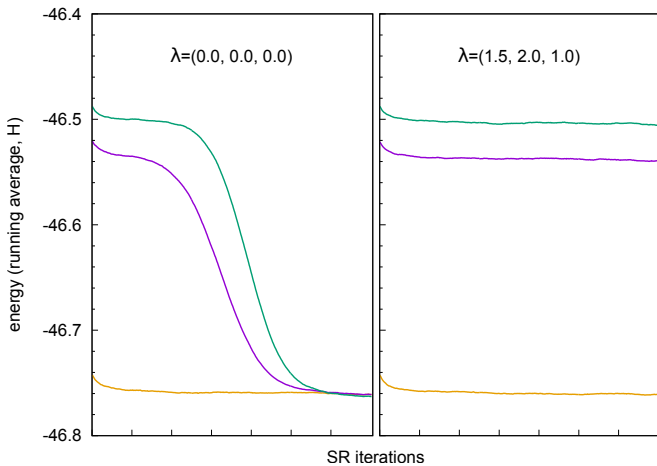


FIG. 1. Plot of the VMC energy during optimization of the 3-state cyclopentadienone system with a CIPSI wave function with 3036 determinants expanded on CAS orbitals. (Left) The collapse of the excited states to the ground state when $\lambda_{IJ} = 0$. (Right) A stable optimization using $\lambda_{12} = 1.5$, $\lambda_{13} = 2.0$, and $\lambda_{23} = 1.0$. The energy points in the plot are calculated from a running average of 100 SR iterations.

In general, the nature of each individual excited state as well as the trial function itself will impact its sensitivity to the value of λ_{IJ} . For instance, in the nitroxyl test case with the 2-determinant wave function (see SI), even with $\lambda_{IJ} = 0$, the excited state still cannot collapse completely to the ground state due to orbital symmetries.

III. COMPUTATIONAL DETAILS

The geometries of nitroxyl, glyoxal, tetrazine, and cyclopentadienone are obtained from ground-state optimizations at the level of CC3/aug-cc-pVTZ.^{12,13} In all calculations we utilize scalar-relativistic energy-consistent Hartree Fock (HF) pseudopotentials⁵⁰ with the corresponding aug-cc-pVDZ Gaussian basis sets. The exponents of the diffuse functions are taken from the corresponding all-electron Dunning's correlation-consistent basis sets⁵¹. For glyoxal, we also tested the use of an aug-cc-pVTZ basis set and found compatible excitation energies both at the VMC and DMC level. All HF and SA-CASSCF calculations are performed in GAMESS(US)⁵² with equal weights on all states.

CIPSI calculations are performed with the Quantum Package^{53,54} program. All states of interest are singlets so determinants are chosen such that the expansions remain eigenstates of \hat{S}^2 with eigenvalue 0. For each molecule, the ground and excited states of interest have the same symmetry so the same set of orbitals are used in all state's determinant expansions. States are weighted and determinants are added to the CIPSI expansion such that the PT2 energy and variance of all states

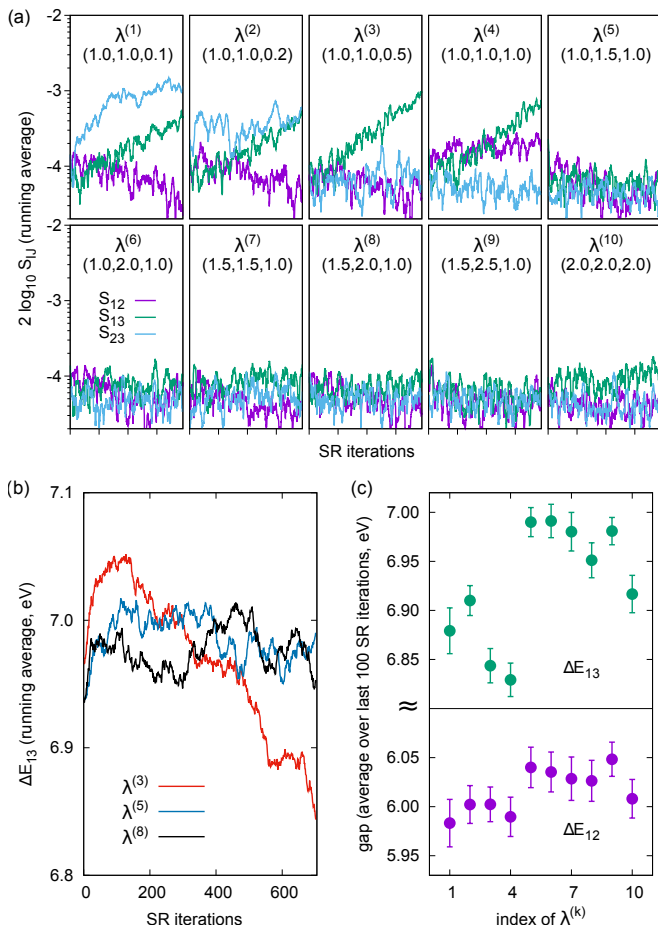


FIG. 2. Effect of λ_{IJ} on the VMC optimization of the 3-state cyclopentadienone system with a CIPSI wave function with 3036 determinants expressed on CAS orbitals. (a) Logarithmic plot of S_{IJ}^2 at each SR iteration for different $\lambda^{(k)} = (\lambda_{12}, \lambda_{13}, \lambda_{23})$. (b) Running average (100 iterations) of ΔE_{13} for three different $\lambda^{(k)}$. (c) The excitation energies averaged over the last 100 SR iterations for each $\lambda^{(k)}$.

remain similar as this has been shown to give more accurate QMC excitation energies.^{34–36} The choice of weights in the CIPSI selection criterion is detailed for each molecule in the SI.

QMC calculations are performed with the CHAMP⁵⁵ program using the method detailed in Section II B. Damping parameters ranging from $\tau_{\text{SR}} = 0.05$ – 0.025 a.u. are used in the SR method during the VMC optimization. A low-memory conjugate-gradient algorithm⁵⁶ is used to solve for the wave function parameters in the SR equations. All DMC calculations use a time-step of $\tau_{\text{DMC}} = 0.02$ a.u.

A value of $\lambda_{IJ} = 1.0$ a.u. is used for all 2-state calculations while multiple values are used for the 3-state system as discussed in the previous Section and in the SI.

IV. RESULTS

A. Nitroxyl $1^1A' \rightarrow 2^1A'$ Double Excitation

This transition in nitroxyl is a pure double $(n, n) \rightarrow (\pi^*, \pi^*)$ excitation. The VMC and DMC energies and VTEs are shown in Table I. There are reliable benchmark calculations for the $1^1A' \rightarrow 2^1A'$ VTE in nitroxyl. In particular, the exFCI/aug-cc-pVQZ (AVQZ) calculation predicts the lowest value for this excitation at 4.32 eV. The latest¹⁶ CC4 and CCSDTQ calculations using the aug-cc-pVTZ (AVTZ) basis set somewhat overestimate it at 4.380 and 4.364 eV, respectively.

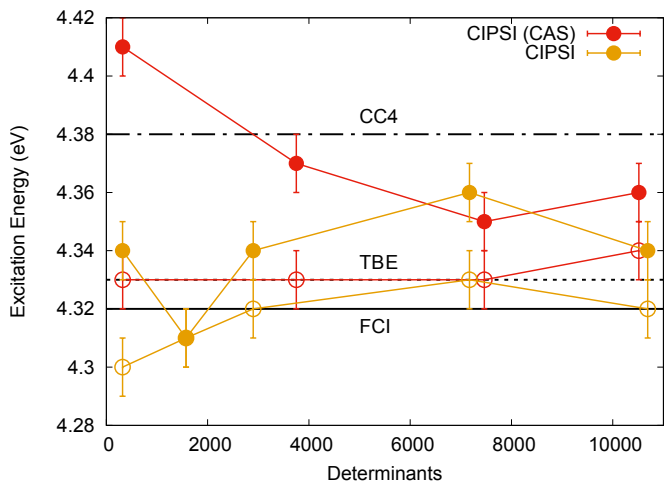


FIG. 3. Nitroxyl VMC (filled points) and DMC (empty points) excitation energies for different CIPSI wave functions expanded either on starting CAS [SA(2)-CASSCF(12,9)] or NO basis, and fully reoptimized in VMC. Horizontal lines represent reference values. TBE: FCI/ATVZ, FCI: exFCI/AVQZ, CC4: CC4/AVTZ.

CIPSI wave functions are expanded in a CAS orbital basis [SA(2)-CASSCF(12,9)] as well as in an NO basis, while matching the PT2 energies and variance. Upon state-specific optimization of the Jastrow-CIPSI wave functions, the VMC and DMC VTEs are very similar for different matching and orbital basis (see Figure 3 and SI) and all are in very good agreement with benchmarks. In addition, consistency of VMC with the DMC excitation energy is reached at fairly small determinant expansions ($\sim 2,000$). Due to the fast convergence of the VMC and DMC excitation energies, the use of NOs in the CIPSI expansion is not necessary, but still provides similar results.

Previous results for nitroxyl show that at least CC4 and CCSDTQ is necessary to capture the important correlations of the $1^1A' \rightarrow 2^1A'$ double excitation. There is also a strong basis set dependence on the excitation with CC methods, yet the VMC and DMC calculations starting from AVDZ with pseudopotentials, reach agreement with expensive quantum chemistry calculations which require the use of at least AVTZ basis set.

TABLE I. Nitroxyl VMC and DMC total energies (a.u.) and excitation energies (eV). The number of determinants (# det) and parameters (# parm) in each trial wave function are also listed. The CIPSI expansions are performed on a NO basis and fully reoptimized in VMC.

WF	# det	# parm	VMC			DMC		
			$E(1^1A')$	$E(2^1A')$	ΔE	$E(1^1A')$	$E(2^1A')$	ΔE
CIPSI	321	850	-26.4917(2)	-26.3322(2)	4.34(1)	-26.5164(2)	-26.3583(2)	4.30(1)
	1573	1446	-26.5001(2)	-26.3415(2)	4.31(1)	-26.5220(2)	-26.3636(2)	4.31(1)
	2900	2002	-26.5040(2)	-26.3447(2)	4.34(1)	-26.5240(2)	-26.3652(2)	4.32(1)
	7171	4124	-26.5102(2)	-26.3498(2)	4.36(1)	-26.5267(2)	-26.3677(2)	4.33(1)
	10690	5712	-26.5113(2)	-26.3519(2)	4.34(1)	-26.5273(2)	-26.3686(2)	4.32(1)
TBE ^a								4.33
CC3/AVQZ ^b								5.23
CC4/AVDZ ^c								4.454
CC4/AVTZ ^c								4.380
CCSDT/AVDZ ^b								4.756
CCSDTQ/AVDZ ^b								4.424
CCSDTQ/AVTZ ^c								4.364
exFCI/AVQZ ^d								4.32(0)
CASPT2(12,9)/AVQZ ^d								4.34
PC-NEVPT2(12,9)/AVQZ ^d								4.35

^aValue is 'safe', as defined in Ref. 12. FCI/AVTZ

^bRef. 15.

^cRef. 16.

^dRef. 13.

B. Glyoxal $1^1A_g \rightarrow 2^1A_g$ Double Excitation

The pure double excitation in glyoxal also corresponds to a $(n, n) \rightarrow (\pi^*, \pi^*)$ transition. Since the system size is larger compared to nitroxyl, the same level of CC4 and CCSDTQ calculations is not available, and there appears to be a large basis set dependence on the most recent CC4 data.¹⁶ A symmetry adapted cluster CI (SAC-CI) calculation of this excitation is available⁵⁷ (5.66 eV) and agrees well with the recent TBE, which is a basis set corrected FCI/AVDZ value of 5.61 eV.¹² These values also agree well with the highest level CCSDTQ estimate for this VTE, 5.670 eV,¹⁶ all shown and compared to our QMC results in Table II.

PT2 and variance-matched CIPSI expansions are generated from the optimal orbitals of a SA(2)-CASSCF(14,12) calculation. As shown in Figure 4, after the optimization of the CIPSI (CAS) wave functions, we observe a somewhat difficult convergence of the excitation energy as the determinant expansion is increased from ~ 400 to $\sim 10,000$. The DMC values tend to also increase, although less dramatically.

When using NOs built from modest-sized CIPSI expansions (10^4 determinants) and re-performing the CIPSI expansions in the presence of the Jastrow factor, the VMC and DMC excitation energies appear to converge nicely and to a value in agreement with available benchmarks. It is possible that still larger CIPSI expansions and more rounds of NO generation could bring the VMC into better alignment with the DMC, which differs at most by 0.05 eV. The DMC value for the largest determinant expansion in the NO basis is 5.63(1) eV, which is ~ 0.01 eV from the current TBE value and ~ 0.02 eV from the SAC-CI/AVDZ and CC4/AVDZ values. This close agreement and the consistency of the DMC results with different number of determinants in the CIPSI wave functions

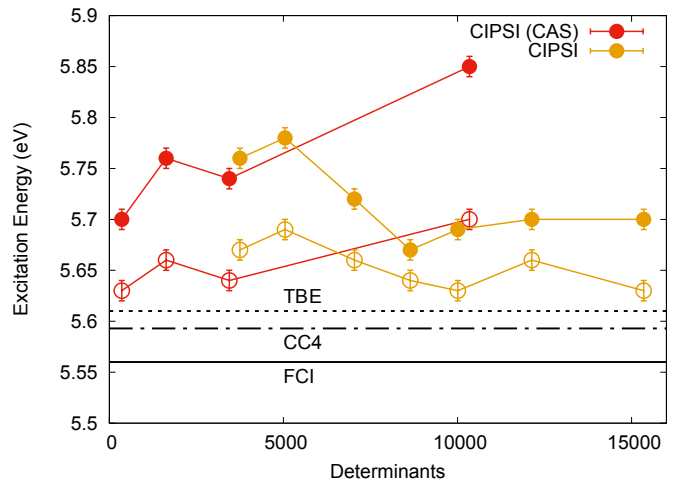


FIG. 4. Glyoxal VMC (filled circles) and DMC (empty circles) excitation energies for different CIPSI wave functions expanded either on starting CAS [SA(2)-CASSCF(14,12)] or NO basis and fully reoptimized in VMC. Horizontal lines represent reference values. TBE: FCI/AVDZ + (CCSDT/AVTZ - CCSDT/AVDZ), CC4: CC4/AVDZ, FCI: exFCI/AVDZ (error bar of ± 0.11 eV).

suggests the value of 5.63(1) eV to be a reasonable prediction for this excitation.

C. Tetrazine $1^1A_{1g} \rightarrow 2^1A_{1g}$ Double Excitation

The tetrazine (*s*-tetrazine) pure double excitation of interest is another $(n, n) \rightarrow (\pi^*, \pi^*)$ transition. There are few reliable benchmark calculations available for this transition due to the

TABLE II. Glyoxal VMC and DMC total energies (a.u.) and excitation energies (eV). The number of determinants (# det) and parameters (# parm) in each trial wave function are also presented. The CIPSI expansions are performed on a NO basis and fully reoptimized in VMC.

WF	# det	# parm	VMC			DMC		
			$E(1^1A_g)$	$E(2^1A_g)$	ΔE	$E(1^1A_g)$	$E(2^1A_g)$	ΔE
CIPSI	3749	2908	-44.6072(2)	-44.3957(2)	5.76(1)	-44.6564(2)	-44.4482(2)	5.67(1)
	5046	3498	-44.6127(2)	-44.4004(2)	5.78(1)	-44.6600(2)	-44.4509(2)	5.69(1)
	7040	4500	-44.6150(2)	-44.4048(2)	5.72(1)	-44.6613(2)	-44.4534(2)	5.66(1)
	8642	5433	-44.6181(2)	-44.4098(2)	5.67(1)	-44.6632(2)	-44.4559(2)	5.64(1)
	10010	6188	-44.6205(2)	-44.4114(2)	5.69(1)	-44.6635(2)	-44.4567(2)	5.63(1)
	12132	6269	-44.6237(2)	-44.4145(2)	5.70(1)	-44.6654(2)	-44.4576(2)	5.66(1)
	15349	8577	-44.6276(2)	-44.4180(2)	5.70(1)	-44.6670(2)	-44.4600(2)	5.63(1)
TBE ^a								5.61
CC3/AVQZ ^b								6.76
CC4/6-31+G* ^c								5.699
CC4/AVDZ ^c								5.593
CCSDTQ/6-31+G* ^c								5.670
exFCI/AVDZ								5.56(11)
SAC-CI/AVDZ ^d								5.66
CASPT2(14,12)/AVQZ ^b								5.43
PC-NEVPT2(14,12)/AVQZ ^b								5.52

^aThis value is ‘safe’, as defined in Ref. 12. exFCI/AVDZ + (CCSDT/AVTZ-CCSDT/AVDZ)

^bRef. 13.

^cRef. 16.

^dRef. 57. See reference for basis set details.

TABLE III. Tetrazine VMC and DMC total energies (a.u.) and excitation energies (eV). The number of determinants (# det) and parameters (# parm) in each trial wave function are also presented. The CIPSI expansions are performed on a NO basis and fully optimized in VMC.

WF	# det	# parm	VMC			DMC		
			$E(1^1A_{1g})$	$E(2^1A_{1g})$	ΔE	$E(1^1A_{1g})$	$E(2^1A_{1g})$	ΔE
CIPSI	3572	2414	-52.2198(2)	-52.0346(2)	5.04(1)	-52.2935(3)	-52.1098(3)	5.00(1)
	7025	4141	-52.2300(2)	-52.0451(2)	5.03(1)	-52.2981(3)	-52.1148(3)	4.99(1)
	10723	6053	-52.2379(2)	-52.0528(2)	5.04(1)	-52.3015(3)	-52.1182(3)	4.99(1)
TBE ^a								4.61
CC3/6-31+G* ^b								6.22
CC3/AVQZ ^b								6.19
CC4/6-31+G* ^c								5.06
CCSDT/AVTZ ^b								5.96
exFCI/AVDZ								5.15(3)
CASPT2(14,10)/AVQZ ^b								4.68
PC-NEVPT2(14,10)/AVQZ ^b								4.60

^aThis value is ‘unsafe’, as defined in Ref 12. NEVTPT2/AVTZ

^bRef. 13.

^cRef. 16.

molecule’s size in addition to its genuine double nature. Although CC3 does not properly treat double excitations, calculations using 6-31+G* up to AVQZ show that there is very little basis set effect, only a change of ~ 0.03 eV on the excitation energy. If the CC4/6-31+G* value of 5.06 eV is just as similar for larger basis sets, then this value can be seen as a good guess for the VTE. In any case, without the calculations available to be sure, the VMC and DMC presented in Table III suggest a value close to 5.0 eV for the VTE.

The VMC optimization of the CAS orbital-based [SA(2)-CASSCF(14,10)] CIPSI expansions tends towards 4.94(1) eV (see SI) while the NO based CIPSI goes to 5.04(1) eV, both converging after about 3,600–3,700 determinants. While the converged VMC excitations energies are not quite in agree-

ment, their DMC values are consistent, with VTEs of 4.97(1) and 4.99(1) eV at the largest determinant expansions (see Figure 5). Even more so than in glyoxal, the consistency of the DMC value for the CIPSI expansions of different length and initial MO basis suggests it should be a trusted benchmark for this transition.

D. 3-State VMC Optimization: Cyclopentadienone $1^1A_1 \rightarrow 2^1A_1$ and $1^1A_1 \rightarrow 3^1A_1$ Excitations

To show the capabilities of the VMC optimization method, the three lowest 1^1A_1 states of cyclopentadienone are optimized simultaneously to determine the two lowest excitation

TABLE IV. Cyclopentadienone VMC and DMC excitation energies (eV). The number of determinants (# det) and parameters (# parm) in each trial wave function is also listed. The CIPSI expansions are performed on a NO basis and fully optimized in VMC. Reference values for the double and single excitation are placed in the ΔE_{12} and ΔE_{13} columns, respectively, to match the order of the states calculated with VMC and DMC. The VMC optimization of the two smaller CIPSI used $\lambda_{i,j}=(1.5,2.0,1.0)$ and, of the two larger, $(1.0,1.0,1.0)$.

WF	# det	# parm	VMC			DMC		
			ΔE_{12}	ΔE_{13}	ΔE_{23}	ΔE_{12}	ΔE_{13}	ΔE_{23}
CIPSI	1025	2403	5.94(1)	6.92(1)	0.98(1)	5.90(1)	6.87(1)	0.97(1)
	3033	3645	5.95(1)	6.96(1)	1.01(1)	5.87(1)	6.87(1)	1.00(1)
	7151	5365	6.03(1)	7.05(1)	1.02(1)	5.92(1)	6.91(1)	0.99(1)
	10206	6574	6.04(1)	7.03(1)	0.99(1)	5.90(1)	6.89(1)	0.99(1)
TBE ^a						6.00 ^b	6.09 ^c	0.09
ADC(3)/AVTZ						4.59 ^d	6.50 ^d	1.91
CC2/AVTZ							6.50 ^d	
CC3/AVTZ						7.10 ^d	6.21 ^d	-0.89
CCSD/AVTZ							6.68 ^d	
CCSDT-3/AVTZ							6.33 ^d	
exFCI/AVDZ						5.81(39)	6.93(24)	1.10(13)

^aThis value is ‘unsafe’ as defined in Ref. 12.

^bNEVPT2/AVTZ.

^cCCSDT/AVDZ + (CC3/AVTZ-CC3/AVDZ).

^dValues are also ‘unsafe’.

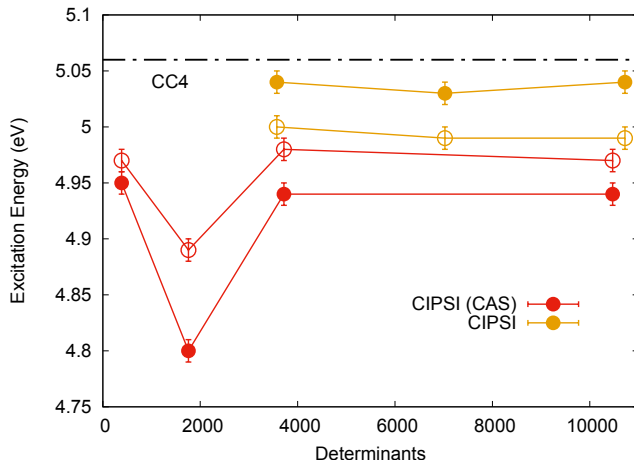


FIG. 5. Tetrazine VMC (filled circles) and DMC (empty circles) excitations energies for different CIPSI wave functions expanded either on starting CAS [SA(2)-CASSCF(14,10)] or NO basis, and fully reoptimized in VMC. Horizontal lines represent the reference value. CC4: CC4/6-31+G*.

energies. One is deemed a double excitation ($\pi, \pi \rightarrow \pi^*, \pi^*$) with $\sim 50\%$ T_1 , and the other a single excitation ($\pi \rightarrow \pi^*$) with $\sim 74\%$ T_1 by CC3 calculations. All results are collected in Table IV.

CC3/AVTZ predicts a value of 7.10 eV for the double excitation and 6.21 eV for the single excitation, which is the opposite of what is found here. The CC3 value for the double excitation is not trustable since it misses quadruple excitations important to describing this type of excitation. Veril et al.¹² determine the CC3 and CCSDT calculations of these excitations to be ‘unsafe’ since they do not agree to within 0.03–0.04 eV. The relatively low T_1 of the single excitation could lead to a poor treatment by CC3 and CCSDT. No CC4

or CCSDTQ calculations are currently available for reliable comparison to the present results for the double excitation energy, and all benchmark VTEs in Table IV are considered unsafe. An exFCI/AVDZ calculation is performed in the present work, although it has fairly large error bars.

All VMC and DMC performed on CIPSI wave functions give roughly the same results (see Table IV, Figure 6, and SI). The largest CIPSI wave function in the NO basis has DMC ΔE_{12} , ΔE_{13} , and ΔE_{23} values of 5.90(1) eV, 6.89(1) eV, and 0.99 eV, respectively.

The present calculations definitively show the ordering of the two lowest 1A_1 excited states. The largest CIPSI calculation performed in the CAS orbital basis [SA(3)-CASSCF(6,6)] finds the 2^1A_1 state to have coefficients of 0.70 and 0.46 for the dominant doubly [$(\pi, \pi) \rightarrow (\pi^*, \pi^*)$] and singly excited ($\pi \rightarrow \pi^*$) CSFs, respectively, while the 3^1A_1 state has coefficients of 0.49 and 0.75. The coefficients show a clear mixing of singly and doubly excited determinants in both states (also suggested by the T_1 values), but the 2^1A_1 state is clearly distinguishable as the double excitation and the 3^1A_1 state as the single.

V. CONCLUSIONS

With the use of a penalty-based, state-specific optimization scheme, we show that the same QMC method which provides accurate single-excitations energies can also be applied to double-excitations. That is, we use PT2 energy and variance matched CIPSI determinant expansions as the Slater part of the Jastrow-Slater trial function in the VMC optimization. The introduction of an objective function allows a state-specific optimization of multiple states of the same symmetry simultaneously by imposing orthogonality between all eigenstates.

For optimization with two states, it is sufficient to apply

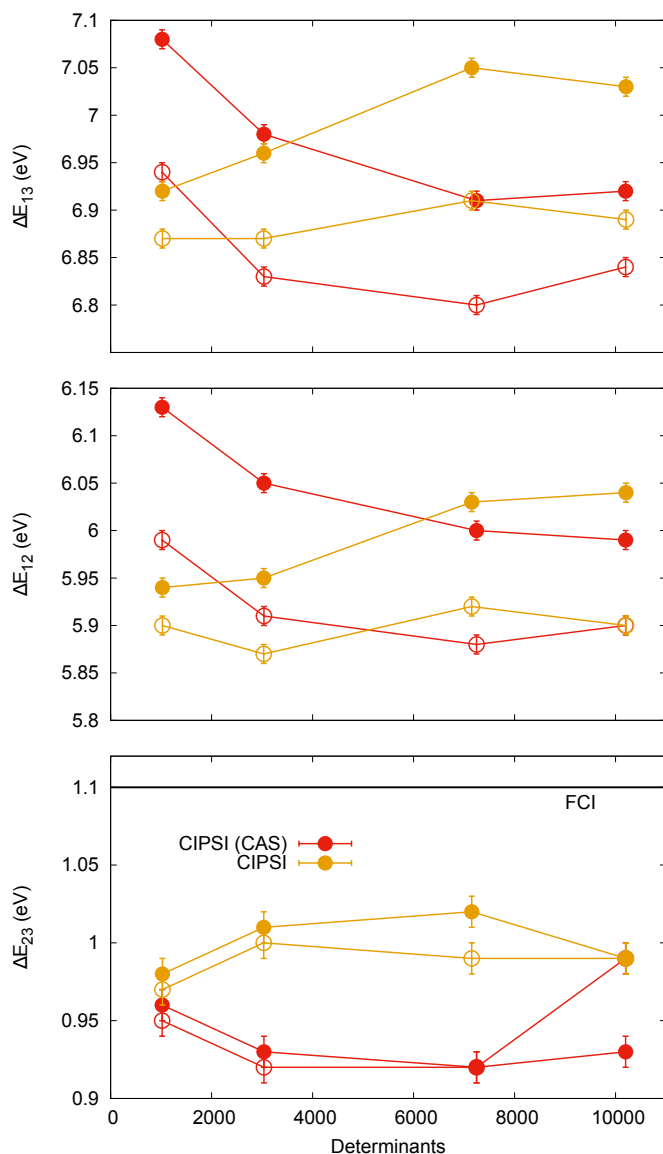


FIG. 6. Cyclopentadienone VMC (filled circles) and DMC (empty circles) excitations energies for different CIPSI wave functions expanded either on starting CAS [SA(3)-CASSCF(6,6)] or NO basis, and fully optimized in VMC. FCI: exFCI/AVDZ (error bar of ± 0.13 eV).

a large enough λ_{12} to stabilize the optimization. With more states, there are wide ranges of the various λ_{IJ} which give consistent and stable excitation energies. Good values can be found at a preliminary stage with relatively few iterations.

The pure double excitations in nitroxyl [4.32(1) eV] and glyoxal [5.63(1) eV] calculated here are in excellent agreement with reliable benchmarks in the literature. We also expect that our VTEs calculated at the level of DMC are reliable benchmarks for molecules and excitation types where CC methods are too costly to do with a large enough basis set. Specifically, we suspect a CC4 calculation with a larger basis set will find a tetrazine double excitation close to our result, 4.99(1) eV, slightly lower than the CC4/6-31G* result. For cy-

clopenta-1,3-dienone, the 1A_1 first excited state ($2{}^1A_1$) is predominantly a double excitation at 5.90(1) eV, while the second excited state is predominantly a single excitation at 6.89(1) eV.

The favorable computational scaling of QMC with the system size and its alignment with modern supercomputers makes it a serious candidate for applications involving complex excited states, such as long range charge-transfer excitations, conical intersections, or problems where the ordering between excited states of different character is unclear.

ACKNOWLEDGMENTS

We thank Pierre-François Loos for useful discussions. This work was supported by the European Centre of Excellence in Exascale Computing TREX — Targeting Real Chemical Accuracy at the Exascale. This project has received funding from the European Union’s Horizon 2020 — Research and Innovation program — under grant agreement no. 952165. The calculations were carried out on the Dutch national supercomputer Cartesius with the support of SURF Cooperative.

- ¹D. P. Chong, *Recent Advances in Density Functional Methods* (WORLD SCIENTIFIC, 1995) <https://www.worldscientific.com/doi/pdf/10.1142/2914>.
- ²K. Burke, J. Werschnik, and E. K. U. Gross, “Time-dependent density functional theory: Past, present, and future,” *The Journal of Chemical Physics* **123**, 062206 (2005), <https://doi.org/10.1063/1.1904586>.
- ³E. Runge and E. K. U. Gross, “Density-functional theory for time-dependent systems,” *Phys. Rev. Lett.* **52**, 997–1000 (1984).
- ⁴A. I. Krylov, “Equation-of-motion coupled-cluster methods for open-shell and electronically excited species: The hitchhiker’s guide to fock space,” *Annual Review of Physical Chemistry* **59**, 433–462 (2008), pMID: 18173379, <https://doi.org/10.1146/annurev.physchem.59.032607.093602>.
- ⁵N. T. Maitra, F. Zhang, R. J. Cave, and K. Burke, “Double excitations within time-dependent density functional theory linear response,” *The Journal of Chemical Physics* **120**, 5932–5937 (2004), <https://doi.org/10.1063/1.1651060>.
- ⁶P. Elliott, S. Goldson, C. Canahui, and N. T. Maitra, “Perspectives on double-excitations in tddft,” *Chemical Physics* **391**, 110–119 (2011), open problems and new solutions in time dependent density functional theory.
- ⁷Y. Shao, M. Head-Gordon, and A. I. Krylov, “The spin-flip approach within time-dependent density functional theory: Theory and applications to diradicals,” *J. Chem. Phys.* **118**, 4807 (2003).
- ⁸F. Wang and T. Ziegler, “Time-dependent density functional theory based on a noncollinear formulation of the exchange-correlation potential,” *J. Chem. Phys.* **121**, 12191 (2004).
- ⁹F. Wang and T. Ziegler, “The performance of time-dependent density functional theory based on a noncollinear exchange-correlation potential in the calculations of excitation energies,” *J. Chem. Phys.* **122**, 074109 (2005).
- ¹⁰Z. Rinkevicius, O. Vahtras, and H. Ågren, “Spin-flip time dependent density functional theory applied to excited states with single, double, or mixed electron excitation character,” *J. Chem. Phys.* **133**, 114104 (2010).
- ¹¹S. Hirata, M. Nooijen, and R. J. Bartlett, “High-order determinantal equation-of-motion coupled-cluster calculations for electronic excited states,” *Chemical Physics Letters* **326**, 255–262 (2000).
- ¹²M. Vénil, A. Scemama, M. Caffarel, F. Lipparini, M. Boggio-Pasqua, D. Jacquemin, and P.-F. Loos, “Questdb: A database of highly accurate excitation energies for the electronic structure community,” *WIREs Computational Molecular Science* **11**, e1517 (2021), <https://wires.onlinelibrary.wiley.com/doi/pdf/10.1002/wcms.1517>.
- ¹³P.-F. Loos, M. Boggio-Pasqua, A. Scemama, M. Caffarel, and D. Jacquemin, “Reference energies for double excitations,” *Journal of Chemical Theory and Computation* **15**, 1939–1956 (2019).
- ¹⁴P.-F. Loos, F. Lipparini, M. Boggio-Pasqua, A. Scemama, and D. Jacquemin, “A mountaineering strategy to excited states: Highly accurate energies and benchmarks for medium sized molecules,” *Journal*

- of Chemical Theory and Computation **16**, 1711–1741 (2020), pMID: 31986042, <https://doi.org/10.1021/acs.jctc.9b01216>.
- ¹⁵P.-F. Loos, D. A. Matthews, F. Lipparini, and D. Jacquemin, “How accurate are eom-cc4 vertical excitation energies?” *Journal of Chemical Physics* **154**, 221103 (2021).
- ¹⁶P.-F. Loos, F. Lipparini, D. A. Matthews, A. Blondel, and D. Jacquemin, “A mountaineering strategy to excited states: Revising reference values with eom-cc4,” (2022).
- ¹⁷H. Koch, O. Christiansen, P. Jørgensen, A. M. Sanchez de Merás, and T. Helgaker, “The cc3 model: An iterative coupled cluster approach including connected triples,” *The Journal of Chemical Physics* **106**, 1808–1818 (1997), <https://doi.org/10.1063/1.473322>.
- ¹⁸J. Noga and R. J. Bartlett, “The full ccsdt model for molecular electronic structure,” *The Journal of Chemical Physics* **86**, 7041–7050 (1987), <https://doi.org/10.1063/1.452353>.
- ¹⁹M. Kállay and J. Gauss, “Approximate treatment of higher excitations in coupled-cluster theory,” *The Journal of Chemical Physics* **123**, 214105 (2005), <https://doi.org/10.1063/1.2121589>.
- ²⁰S. A. Kucharski and R. J. Bartlett, “Recursive intermediate factorization and complete computational linearization of the coupled-cluster single, double, triple, and quadruple excitation equations,” *Theoretica chimica acta* **80**, 387–405 (1991).
- ²¹K. Andersson, P. A. Malmqvist, B. O. Roos, A. J. Sadlej, and K. Wolinski, “Second-order perturbation theory with a ccsf reference function,” *The Journal of Physical Chemistry* **94**, 5483–5488 (1990), <https://doi.org/10.1021/j100377a012>.
- ²²C. Angeli, R. Cimiraglia, and J.-P. Malrieu, “N-electron valence state perturbation theory: a fast implementation of the strongly contracted variant,” *Chemical Physics Letters* **350**, 297–305 (2001).
- ²³J. P. Zobel, J. J. Nogueira, and L. González, “The ipea dilemma in caspt2,” *Chem. Sci.* **8**, 1482–1499 (2017).
- ²⁴B. Huron, J. P. Malrieu, and P. Rancurel, “Iterative perturbation calculations of ground and excited state energies from multiconfigurational zeroth-order wavefunctions,” *The Journal of Chemical Physics* **58**, 5745–5759 (1973), <https://doi.org/10.1063/1.1679199>.
- ²⁵A. Povill, J. Rubio, and F. Illas, “Treating large intermediate spaces in the cipsi method through a direct selected ci algorithm,” *Theoretica Chimica Acta* **82**, 229–238 (1992), <https://doi.org/10.1007/BF01113255>.
- ²⁶P. M. Zimmerman, “Incremental full configuration interaction,” *The Journal of Chemical Physics* **146**, 104102 (2017), <https://doi.org/10.1063/1.4977727>.
- ²⁷W. M. C. Foulkes, L. Mitas, R. J. Needs, and G. Rajagopal, “Quantum monte carlo simulations of solids,” *Rev. Mod. Phys.* **73**, 33–83 (2001).
- ²⁸A. Lüchow, “Quantum monte carlo methods,” *WIREs Computational Molecular Science* **1**, 388–402 (2011), <https://wires.onlinelibrary.wiley.com/doi/pdf/10.1002/wcms.40>.
- ²⁹B. M. Austin, D. Y. Zubarev, and W. A. Lester, “Quantum monte carlo and related approaches,” *Chemical Reviews* **112**, 263–288 (2012), pMID: 22196085, <https://doi.org/10.1021/cr2001564>.
- ³⁰S. Sorella and L. Capriotti, “Algorithmic differentiation and the calculation of forces by quantum monte carlo,” *The Journal of Chemical Physics* **133**, 234111 (2010), <https://doi.org/10.1063/1.3516208>.
- ³¹C. Filippi, R. Assaraf, and S. Moroni, “Simple formalism for efficient derivatives and multi-determinant expansions in quantum monte carlo,” *The Journal of Chemical Physics* **144**, 194105 (2016), <https://doi.org/10.1063/1.4948778>.
- ³²R. Assaraf, S. Moroni, and C. Filippi, “Optimizing the energy with quantum monte carlo: A lower numerical scaling for jastrow–slater expansions,” *Journal of Chemical Theory and Computation* **13**, 5273–5281 (2017), pMID: 28873307, <https://doi.org/10.1021/acs.jctc.7b00648>.
- ³³A. Ammar, E. Giner, and A. Scemama, “Optimization of large determinant expansions in quantum Monte Carlo,” *arXiv* (2022), [10.48550/arXiv.2205.12851](https://arxiv.org/abs/10.48550/arXiv.2205.12851), 2205.12851.
- ³⁴M. Dash, J. Feldt, S. Moroni, A. Scemama, and C. Filippi, “Excited states with selected configuration interaction-quantum monte carlo: Chemically accurate excitation energies and geometries,” *Journal of Chemical Theory and Computation* **15**, 4896–4906 (2019), pMID: 31348645, <https://doi.org/10.1021/acs.jctc.9b00476>.
- ³⁵A. Cuzzocrea, A. Scemama, W. J. Briels, S. Moroni, and C. Filippi, “Variational principles in quantum monte carlo: The troubled story of variance minimization,” *Journal of Chemical Theory and Computation* **16**, 4203–4212 (2020), pMID: 32419451, <https://doi.org/10.1021/acs.jctc.0c00147>.
- ³⁶M. Dash, S. Moroni, C. Filippi, and A. Scemama, “Tailoring cipsi expansions for qmc calculations of electronic excitations: The case study of thiophene,” *J. Chem. Theory Comput.* **17**, 3426–3434 (2021).
- ³⁷C. Filippi, M. Zacccheddu, and F. Buda, “Absorption spectrum of the green fluorescent protein chromophore: A difficult case for ab initio methods?” *Journal of Chemical Theory and Computation* **5**, 2074–2087 (2009), pMID: 26613149, <https://doi.org/10.1021/ct900227j>.
- ³⁸P. M. Zimmerman, J. Toulouse, Z. Zhang, C. B. Musgrave, and C. J. Umrigar, “Excited states of methylene from quantum monte carlo,” *The Journal of Chemical Physics* **131**, 124103 (2009), <https://doi.org/10.1063/1.3220671>.
- ³⁹O. Valsson and C. Filippi, “Photoisomerization of model retinal chromophores: Insight from quantum monte carlo and multiconfigurational perturbation theory,” *Journal of Chemical Theory and Computation* **6**, 1275–1292 (2010), <https://doi.org/10.1021/ct900692y>.
- ⁴⁰R. Send, O. Valsson, and C. Filippi, “Electronic excitations of simple cyanine dyes: Reconciling density functional and wave function methods,” *Journal of Chemical Theory and Computation* **7**, 444–455 (2011), pMID: 26596164, <https://doi.org/10.1021/ct1006295>.
- ⁴¹O. Valsson, P. Campomanes, I. Tavernelli, U. Rothlisberger, and C. Filippi, “Rhodopsin absorption from first principles: Bypassing common pitfalls,” *Journal of Chemical Theory and Computation* **9**, 2441–2454 (2013), pMID: 26583734, <https://doi.org/10.1021/ct3010408>.
- ⁴²R. Guareschi, H. Zulfikri, C. Daday, F. M. Floris, C. Amovilli, B. Menucci, and C. Filippi, “Introducing qmc/mmpol: Quantum monte carlo in polarizable force fields for excited states,” *Journal of Chemical Theory and Computation* **12**, 1674–1683 (2016), pMID: 26959751, <https://doi.org/10.1021/acs.jctc.6b00044>.
- ⁴³R. J. Hunt, M. Szyniszewski, G. I. Prayogo, R. Maezono, and N. D. Drummond, “Quantum monte carlo calculations of energy gaps from first principles,” *Phys. Rev. B* **98**, 075122 (2018).
- ⁴⁴N. S. Blunt and E. Neuscamman, “Excited-state diffusion monte carlo calculations: A simple and efficient two-determinant ansatz,” *Journal of Chemical Theory and Computation* **15**, 178–189 (2019), <https://doi.org/10.1021/acs.jctc.8b00879>.
- ⁴⁵N. S. Blunt, S. D. Smart, G. H. Booth, and A. Alavi, “An excited-state approach within full configuration interaction quantum monte carlo,” *The Journal of Chemical Physics* **143**, 134117 (2015), <https://aip.scitation.org/doi/pdf/10.1063/1.4932595>.
- ⁴⁶K. Choo, G. Carleo, N. Regnault, and T. Neupert, “Symmetries and many-body excitations with neural-network quantum states,” *Phys. Rev. Lett.* **121**, 167204 (2018).
- ⁴⁷S. Pathak, B. Busemeyer, J. N. B. Rodrigues, and L. K. Wagner, “Excited states in variational monte carlo using a penalty method,” *The Journal of Chemical Physics* **154**, 034101 (2021), <https://doi.org/10.1063/5.0030949>.
- ⁴⁸S. Sorella, “Generalized lanczos algorithm for variational quantum monte carlo,” *Phys. Rev. B* **64**, 024512 (2001).
- ⁴⁹M. Casula, C. Attaccalite, and S. Sorella, “Correlated geminal wave function for molecules: An efficient resonating valence bond approach,” *The Journal of Chemical Physics* **121**, 7110–7126 (2004), <https://doi.org/10.1063/1.1794632>.
- ⁵⁰M. Burkatzki, C. Filippi, and M. Dolg, “Energy-consistent pseudopotentials for quantum monte carlo calculations,” *The Journal of Chemical Physics* **126**, 234105 (2007), <https://doi.org/10.1063/1.2741534>.
- ⁵¹R. A. Kendall, T. H. Dunning Jr, and R. J. Harrison, “Electron affinities of the first-row atoms revisited. systematic basis sets and wave functions,” *J. Chem. Phys.* **96**, 6796–6806 (1992).
- ⁵²G. M. J. Barca, C. Bertoni, L. Carrington, D. Datta, N. De Silva, J. E. Deustua, D. G. Fedorov, J. R. Gour, A. O. Gunina, E. Guidez, T. Harville, S. Irle, J. Ivanic, K. Kowalski, S. S. Leang, H. Li, W. Li, J. J. Lutz, I. Magoulas, J. Mato, V. Mironov, H. Nakata, B. Q. Pham, P. Piecuch, D. Poole, S. R. Pruitt, A. P. Rendell, L. B. Roskopf, K. Ruedenberg, T. Sattasathuchana, M. W. Schmidt, J. Shen, L. Slipchenko, M. Sosonkina, V. Sundriyal, A. Tiwari, J. L. Galvez Valjejo, B. Westheimer, M. Wloch, P. Xu, F. Zahariev, and M. S. Gordon, “Recent developments in the general atomic and molecular electronic structure system,” *The Journal of Chemical Physics* **152**, 154102 (2020).
- ⁵³Y. Garniron, T. Applencourt, K. Gasperich, A. Benali, A. Ferté,

- J. Paquier, B. Pradines, R. Assaraf, P. Reinhardt, J. Toulouse, P. Barbareco, N. Renon, G. David, J.-P. Malrieu, M. V  ril, M. Caffarel, P.-F. Loos, E. Giner, and A. Scemama, "Quantum package 2.0: An open-source determinant-driven suite of programs," *Journal of Chemical Theory and Computation* **15**, 3591–3609 (2019), pMID: 31082265, <https://doi.org/10.1021/acs.jctc.9b00176>.
- ⁵⁴A. Scemama, M. Caffarel, A. Benali, D. Jacquemin, and P.-F. Loos, "Influence of pseudopotentials on excitation energies from selected configuration interaction and diffusion monte carlo," *Results in Chemistry* **1**, 100002 (2019).
- ⁵⁵CHAMP is a quantum Monte Carlo program package written by C. J. Umrigar, C. Filippi, S. Moroni and collaborators.
- ⁵⁶E. Neuscamman, C. J. Umrigar, and G. K.-L. Chan, "Optimizing large parameter sets in variational quantum monte carlo," *Phys. Rev. B* **85**, 045103 (2012).
- ⁵⁷B. Saha, M. Ehara, and H. Nakatsuji, "Singly and doubly excited states of butadiene, acrolein, and glyoxal: Geometries and electronic spectra," *The Journal of Chemical Physics* **125**, 014316 (2006), <https://doi.org/10.1063/1.2200344>.
- ⁵⁸M. Dash, S. Moroni, A. Scemama, and C. Filippi, "Perturbatively selected configuration-interaction wave functions for efficient geometry optimization in quantum monte carlo," *Journal of Chemical Theory and Computation* **14**, 4176–4182 (2018), pMID: 29953810, <https://doi.org/10.1021/acs.jctc.8b00393>.
- ⁵⁹M. Dash, J. Feldt, S. Moroni, A. Scemama, and C. Filippi, "Excited states with selected configuration interaction-quantum monte carlo: Chemically accurate excitation energies and geometries," *Journal of Chemical Theory and Computation* **15**, 4896–4906 (2019), pMID: 31348645, <https://doi.org/10.1021/acs.jctc.9b00476>.